Prepublished copy

Nature Environment & Pollution Technology

This is a peer-reviewed prepublished version of the paper

Original Research

Superficial Urban Heat Island in the City of Santos/Brazil

Julio Angeles Suazo[1]; Roberto Angeles Vasquez[2]; Carmencita Lavado Meza[1]; Nataly Angeles Suazo[3*]; Leonel de la Cruz Cerrón[4]; Pabel Meza Mitma[1]; Jose Flores Rojas[5] and Hugo Abi Karam[6]

[1] Universidad Nacional Autónoma de Tayacaja Daniel Hernández Morillo. Tayacaja, Perú jangelesambiental@gmail.com

[2] Universidad Nacional del Centro del Perú. Huancayo, Perú, roanvas@hotmail.com

[3] Universidad Tecnológica del Perú. Lima, Perú, nati2643@hotmail.com

[4] Universidad Continental. Huancayo, Perú, ldelacruz@continental.edu.pe

[5] Instituto Geofísico del Perú. Lima, Perú, jflores@igp.gob.pe

[6] Universidade Federal do Rio de Janeiro. Rio de Janeiro, Brazil, hugo@igeo.ufrj.br

Corresponding author: Nataly Angeles Suazo (Universidad Tecnológica del Perú); nati2643@hotmail.com

ORCID IDs of Authors

Julio Angeles Suazo; https://orcid.org/0000-0001-8327-9032

Roberto Angeles Vasquez; https://orcid.org/0000-0002-7248-912X

Carmencita Lavado Meza; https://orcid.org/0000-0003-1620-7180

Nataly Angeles Suazo; https://orcid.org/0000-0001-6144-0673

Leonel de la Cruz Cerrón; https://orcid.org/0000-0003-0935-3075

Pabel Meza Mitma; https://orcid.org/0000-0001-9133-2868

Jose Flores Rojas; https://orcid.org/0000-0002-7205-322X

Hugo Abi Karam; https://orcid.org/0000-0002-0154-5569

Key Words	Heat island, Santos, Brazil, Heat island, Quantiles
DOI	https://doi.org/10.46488/NEPT.2025.v24i04.D1776 (DOI will be active only after the final publication of the paper)
Citation for the Paper	Julio Angeles Suazo, Roberto Angeles Vasquez, Carmencita Lavado Meza, Nataly Angeles Suazo, Leonel de la Cruz Cerrón, Pabel Meza Mitma, Jose Flores Rojas and Hugo Abi Karam., 2025. Superficial Urban Heat Island in the City of Santos/Brazil. *Nature Environment and Pollution Technology*, 24(4), p. D1776. https://doi.org/10.46488/NEPT.2025.v24i04.D1776

ABSTRACT

This contribution estimates the intensity of Urban Heat Island (UHI) during the period 2001 - 2020 for the city of Santos (CS), located in Sao Paulo - Brazil. The formation of the Surface Urban Heat Island (SUHI) was quantified from 2 methods: the first was Streutker's method, which adjusts the surface soil temperature (LST) (urban and rural

surface) to a Gaussian surface. The second, the quantile method proposed by Jose Flores, uses the difference between the 0.95 quantile of the LST of the urban area and the median of the LST of the rural area. Both methods use remote sensing data of LST at 0.050 resolution, obtained from the MODIS sensor on board the TERRA and AQUA satellites. In general, the quantile method can be used as a complementary analysis to the Streutker method for cities with high LST. The results of the CS analysis, during diurnal periods, indicate maximum values in May (5.09°C) and minimum values in August (3.87°C). During the night period, it presented maximum values in February (3.94°C) and minimum values in August (2.40°C) with the quantile method, and due to its proximity to the Small Ocean, the Streutker method presents interferences.

INTRODUCTION

Urbanization produces significant changes in the radiative, thermal and aerodynamic properties of surfaces through the formation of heat domes over cities, called urban heat islands (UHI) (Oke, 1982; Arnfield, 2003). The spatial distribution of UHIs is usually marked by a strong horizontal temperature gradient in the urban-rural boundary zone and a gradual decrease in temperature from the center to the edge of the city, these gradients are strongly affected by local circulation and climatic conditions; therefore, they are defined by diurnal and seasonal variations (Kim and Baik, 2005; Roth, 2007).

The main factors contributing to the formation and development of UHI spatial patterns include: scarcity of vegetation, extensive use of imperviousness, high thermal capacity, albedo of building materials and paving; which reduces evaporation, this generates the typical three-dimensional geometry of urban surfaces (canyon-like configuration). For example, the existence of infrastructures with impermeable materials and thermal characteristics cause a decrease in albedo and an increase in surface temperature, as well as a reduction in relative humidity and evapotranspiration (Oke, 1988; Kuang *et al.*, 2017; Soltani and Sharifi, 2017; Dai, Guldmann and Hu, 2019; Ouyang *et al.*, 2022).

Industrial, human, construction and transportation activities all contribute to the formation of heat islands, significantly affecting the local climate (Shahmohamadi *et al.*, 2011; Wang *et al.*, 2021). Since the urban surface traps the surrounding energy due to its extension, anthropogenic heat release also occurs through vehicle traffic, industrial/human processes, animal metabolism and energy consumption, which generates a high rate of energy absorption due to the concentration of pollutants (gases and aerosols) in the urban atmosphere. In addition, the spatial patterns of UHI can be strongly influenced by the type of surface cover such as: green areas, water bodies and topography (Oke, 1982, 1987; Kolokotroni *et al.*, 2012). There are studies that show that UHI can generate strong increases in surface temperature, low levels of specific humidity and precipitation in urban coastal areas (Holst, Tam and Chan, 2016; Fung *et al.*, 2021; Hu *et al.*, 2021).

The present contribution proposes to estimate the SUHI of city of Santos (CS) at low resolution during the period (2001-2020). The estimation is based on the use of the statistical quantile analysis method of LST data

and the Streutker method, with low resolution data obtained from the MODIS sensor on board the AQUA and TERRA satellites.

2. MATERIALS AND METHODS

The materials and methods are presented in three subsections: one describes where the measurements were made, another section describes the sensor used, and the last section describes the methods used for ICUS estimation.

2.1. Site and location

The city of Santos (CS) is located in the southeast of South America, in Brazil, in the state of Sao Paulo. The state of Sao Paulo is composed of 39 municipalities (one of them called the municipality of Santos), with a total population of 20 million inhabitants, representing 11% of the population of Brazil, and has a relative humidity of 7% and annual accumulated rainfall of 400 mm (Flores R., Pereira Filho and Karam, 2016).

To distinguish the behavior of LST throughout the year, both for urban and rural areas and the relationship of these with vegetation cover, 3 points with different surface coverages were selected for the present study. Fig. 1a shows the rural location identified with (23.89 S, 46.20 W), Urban (23.95 S, 46.37 W) and border (23.94 S, 46.27 W), identified by the letters R, U and B respectively.

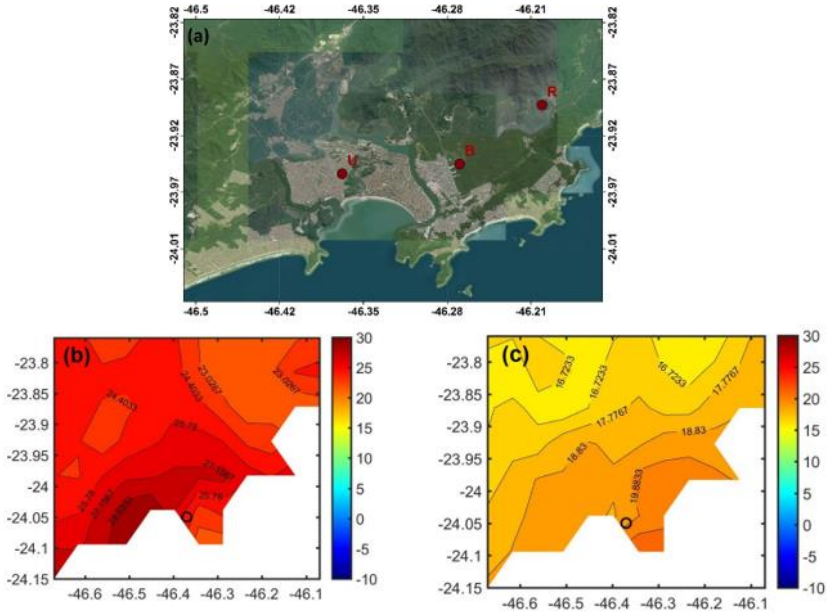

Fig. 1: (a) Area delimited as the CS domain, showing rural R (23.89 S, 46.20 W), Urban U (23.95 S, 46.37 W) and border B (23.94 S, 46.27 W), (b) monthly mean LST during the daytime period and (c) monthly mean LST of the nighttime period, both for December 2001.

2.2. MODIS data

The MODIS sensor of the AQUA and TERRA satellite was used, where the MODIS thermal infrared (TIR) sensors measure radiances of the top of the atmosphere (TOA). These brightness temperatures are different from Land Surface Temperature (LST) with a difference of 1 to 5 K, due to the non-vertical satellite viewing angle, urban geometry, sub-pixel variation of surface temperature, variable surface emissivity and various atmospheric effects (Dousset and Gourmelon, 2003). In addition, MODIS AQUA has a better representation between LST/UHI, unlike other satellites (Zargari *et al.*, 2024).

To remove these effects and estimate LST from space, a MODIS LST day-night method has been designed to take advantage of the unique capability of the MODIS instrument (Wan, 1999). This method uses day-night pairs of TIR data in seven MODIS bands to simultaneously retrieve surface temperatures and band-averaged emissivities in bands 20, 22, 23, 23, 29, and 31-33 without knowing the water vapor and atmospheric temperature profiles with high accuracy (Wan and Li, 1997). In addition, in order to generate more regionally representative urban temperature estimates, three-dimensional roughness of urban surfaces, which depends on satellite imagery, was considered (Voogt and Oke, 2003).

In the present study, monthly averaging and scaling up to 5 km resolution was performed to analyze the effects of rescaling on the LST statistical patterns and then compared to the MOD11C3 Global CMG product, which is a composite monthly average, derived from the MOD11C1 daily global product. These data are stored as clear-sky LST values over a period of months at a resolution of 0.05^0 (5600 meters).

In order to separate urban and rural areas, the MCD12C1 MODIS land cover product type MCD12C1 with 0.050 resolution was used to classify the land surface according to the international Geosphere-Biosphere Project (IGBP), 17 land cover types. In this categorization, an urban category has been obtained from MODIS version 4 observations following the contribution of Schneider (Schneider *et al.*, 2003) (Fig. 2b.).

3.3. SUHI estimation

To determine the SUHI, the Gaussian Method (Streutker, 2003)(Streutker, 2003), and the quantile method (Flores R., Pereira Filho and Karam, 2016) were used, both methods were used in the estimation of urban surface heat island in the cities of Arequipa, Huancayo and Iquitos (e.g. (Suazo, Rojas and Karam, 2020)).

The Streutker Method proposed by Streutker (2002) (Streutker, 2003) was used to determine the SUHI. The technique uses a least-square fit of the entire heat island to a Gaussian surface of the form:

$$T_{(x,y)} = T_0 + a_1 x + a_2 y + a_0 e^{\left(-\frac{(x-x_0)^2}{2a_x^2} - \frac{(y-y_0)^2}{2a_y^2}\right)} \quad \ldots\ldots\ldots (1)$$

Where $T_{(x,y)}$ is the total surface temperature, including urban and rural pixels. T_0, a_1 and a_2 are the costant and linear components of the rural temperature, respectively.

The quantile method proposed by Flores (Flores R., Pereira Filho and Karam, 2016) (Flores R., Pereira Filho and Karam, 2016)to estimate the SUHI intensity, where it is based on the statistical analysis of urban and rural LST quantiles. He also proposed the following formula to estimate the SUHI intensity for a resolution of 5 km:

$$SUHI = Q_5^{urban} - Q_3^{rural} \quad \ldots\ldots\ldots (2)$$

Where Q_5^{urban} is the 0.95 quantile of the LST distribution over the urban area and Q_3^{rural} is the median of the LST distribution over the rural area, both with a resolution of 5 km.

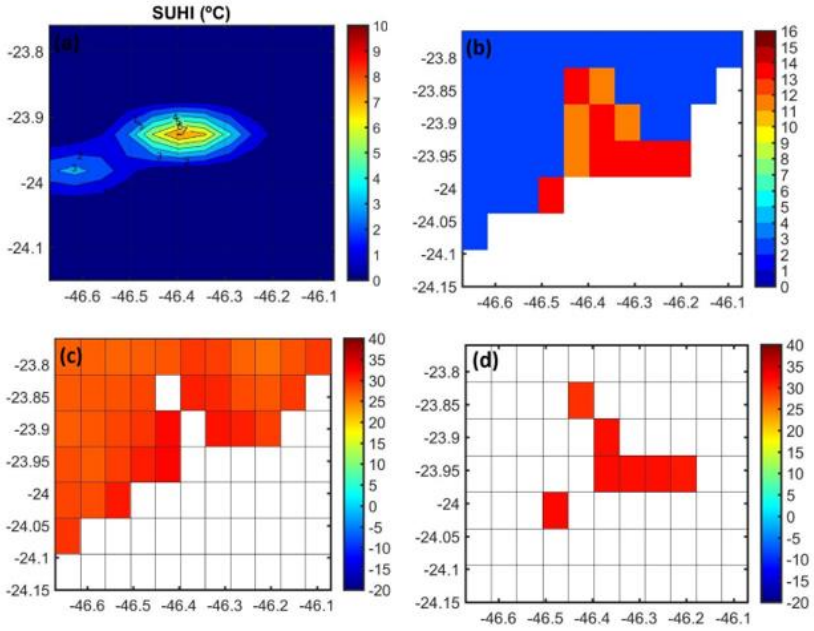

Fig. 2: (a) Least-Squares planar interpolation for rural LST (b) Land cover type for December 2006 according to the IGBP (c) Monthly mean diurnal LST (5km resolution) under the urban area of the MSA for January 2001 (d) Monthly mean diurnal LST of the rural area of the CS for January 2001.

3. RESULTS AND DISCUSSIONS

The results for the long-term (2001-2020) diurnal SUHI magnitudes and spatial extents for all months over the CS using the Streutker method are presented in Table 1. The highest SUHI intensity for the period occurred in November (3.19°C) and the lowest SUHI intensity was observed in January (2.62°C); on the contrary, for Suazo et al. (2019) the maximum values were found in September and the minimum in May. Heat stress, usually in the afternoon, limits daily vitality on the public highway (Soltani and Sharifi, 2017). On the other hand, there is a correlation between the increase in vegetation and colder areas (Anees *et al.*, 2025). Add, high temperatures predominate in the central region of the city and decrease as the distance from the city increases, being lower in the rural areas, as indicated by Novio et al. (2024).

Fig. 3a shows the scatter plot between the two methods for all months. The slope of the linear adjustment of the data is equal to 0.3, the intersection is at point 1.2 and the correlation found between both methods is

equal to 0.12, although they are calculating the same variable, they are not related in terms of their estimation. Likewise, in Fig. 3b for the night period, the linear fit to the data shows a slope equal to 0.63, the intersection is equal to -0.67 and the correlation index is equal to 0.11. However, according to the research of Peng et al. (2024), there are some increasing trend of SUHI in areas with urban expansion during summer; moreover, there are decreasing ranges and intensities of SUHI in areas with high altitude and low economic level, while with high economic level and low altitude there are cities with dominant increases. In addition, LST is negatively correlated with proximity to the coast during the day and positively correlated at night in SUHI studies (Jacobs *et al.*, 2020; You *et al.*, 2021; Chen *et al.*, 2022).

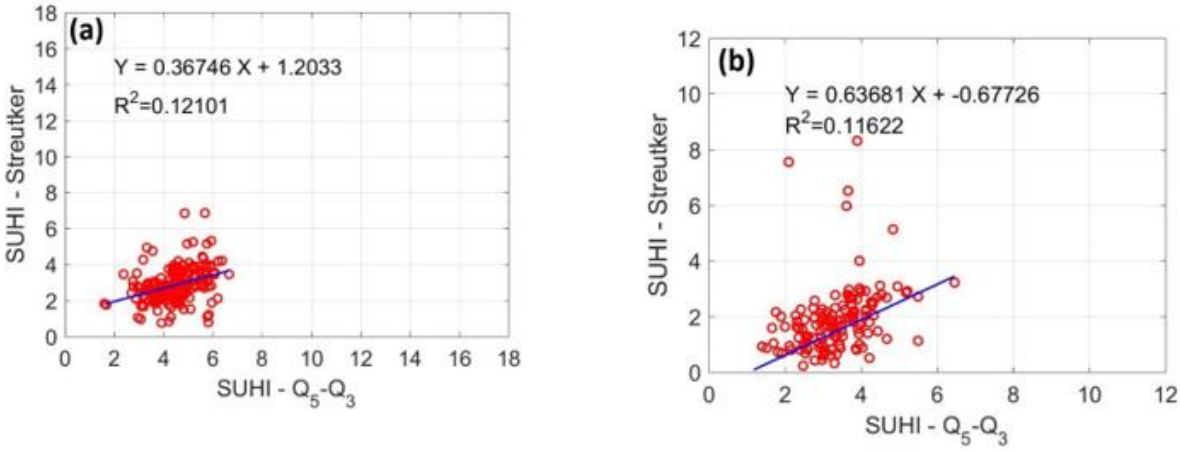

Fig. 3: (a) Scatter-plot of SUHI in diurnal periods, obtained with Streutker's method vs SUHI with the quantile difference Q_5^{urban} and Q_3^{rural} for the MSA, (b) nocturnal period.

For the CS, the results of the SUHI calculation using the statistical method of quantiles and Streutker in diurnal and nocturnal periods are shown in Table 1. The SUHI intensities with the diurnal quantile method present maximum values in May (5.09°C) and minimum values in August (3.87°C). SUHI intensities with the quantile method for the nocturnal period present maximum values in February (3.94°C) and minimum values in August (2.40°C). In general, the Streutker method underestimates the SUHI intensities, this characteristic is best observed during the night period, as demonstrated by Suazo et al. (2019). However, for Ma et al. (2024), they were lower values being 0.97 ± 0.78°C and 0.21 ± 0.87°C during the day and night, respectively, since at high altitudes the nocturnal is slightly higher than the diurnal, due to atmospheric pressure limiting heat reduction and conduction.

On the other hand, in the case of Zargari et al. (2024), higher values have been observed in the suburbs during the day, while at night, in central urban areas; for García (2022), cities near the coast have a higher diurnal temperature (SUHI = 1.44°C, LST = 3.90°C) and decreases as one moves away (SUHI = 0.52°C, LST = 2.85°C); and for Shapiro and Liu (2023), the LST values are higher in coastal areas, being the maximum 36.90°C and 33.55°C in the wet and dry season, respectively, but as it decreases at night. In the case of Wu et

al. (2019), they mention that the distance to the coast does not influence the UHI effect and the vegetation cover is more related to SUHI, both for spring and summer, in addition to the population density.

Furthermore, as mentioned by Hardin et al. (2018), surface characteristics are not the only factor influencing SUHI, as air pollution and meteorological conditions can affect variation, and it should be noted that LST has a relationship with N_2O levels (Suthar *et al.*, 2023); therefore, there are higher values in spring in highly industrialized areas with little vegetation and excessive levels of nitrogen compounds (Kazemi *et al.*, 2025) compared to green spaces (Feizizadeh and Blaschke, 2013). Thus, there is a relationship between air pollutants and surface conditions with SUHIs (Iungman *et al.*, 2024) and urban morphology (Esposito *et al.*, 2024).

Table 1. Daytime and nighttime mean SUHI and spatial extent with standard deviation for the CS using the method developed by Streutker (2002) and Flores (2016) for the period 2001-2020.

MONTHS	SUHI STREUTKER DAYTIME (°C)	SUHI CUANTIL DAYTIME (°C)	SUHI CUANTIL NIGHT(°C)
January	2.62 ± 1.66	4.67 ± 0.76	3.59 ± 0.99
February	2.91 ± 0.81	4.96 ± 0.86	3.94 ± 0.82
March	2.79 ± 0.85	4.26 ± 0.83	3.60 ± 1.10
April	3.05 ± 0.55	4.77 ± 0.79	3.56 ± 0.64
May	3.01 ± 0.69	5.09 ± 0.53	3.32 ± 0.55
Juny	2.52 ± 0.57	4.03 ± 0.73	2.69 ± 0.81
July	2.73 ± 0.59	4.02 ± 0.57	2.44 ± 0.56
August	2.71 ± 0.48	3.87 ± 0.64	2.40 ± 0.46
September	3.05 ± 1.18	4.05 ± 1.09	2.71 ± 0.60
October	3.01 ± 0.84	4.38 ± 1.24	3.46 ± 1.09
November	3.19 ± 1.19	4.74 ± 1.07	3.89 ± 0.53
December	2.31 ± 1.28	3.91 ± 0.99	3.69 ± 0.85

The monthly behavior of the SUHI seen in Fig. 4a and 4b, shows that, although the LST has a strong variation, the SUHI intensities and the monthly variation are little influenced in terms of amplitude, observed for both Streutker and quantile methods. During the night period, the mean rural LST drops significantly, which becomes m the quantile 0.95 (Q_5) of the urban area and the median (Q_3) of the rural area for the CS (Fig. 4b). The main causes that generate these differences between both methods may be the LST pattern over the rural area does not fit well in a straight plane because the pixel is close to Santa Rita lagoon and finally with the small Sea, these water bodies manage to retain large amounts of energy and influence the heat dispersion in the vicinity. An example is the case of Yao et al. (2018), when using nearby suburban areas as a reference background, an underestimation of SUHI of about 1.48°C is generated, while ignoring water bodies and elevation effects with rural area selection leads to an overestimation of SUHI by 1.63°C in 31 cities in China. In addition, as indicated by Du et al. (2025), the identification of LST grid anomalies (LSTA) can be used to decrease the bias by identifying LST anomalies in grid (LSTA) to pinpoint the transition of urban areas. On the other hand, urban

areas with higher building density and minimal vegetation cover are warmer by 1.2°C compared to environments with more open buildings; while natural areas are 2.4°C colder than areas with agglomerated buildings and 1.3°C colder with more open buildings (Suthar *et al.*, 2023). In addition, there are soil indices such as NVDI, NDBI and NDWI that provide a complement to the analysis by LST, to improve the compression of the temperature variation of the UHI (Nandi *et al.*, 2024) and to consider the uncertainty generated by estimating temperature through retrieval algorithms from satellite remote sensing (Hurduc et al., 2024).

In this work as seen in Fig. 2a there are two centers of maximum temperatures, thus the cantile method was useful to perform the complementary analysis of the Streutker method due to the presence of more than one center of maximum surface temperature as suggested by Flores R., Pereira Filho and Karam (2016). Improving the understanding of heat island behavior can help in the formulation of new urban environmental policies and improved public life management focusing on climate change (Soltani and Sharifi, 2017), towards more sustainable and climate-resilient cities in similar urban contexts (Anees *et al.*, 2025). For example, according to Luo et al. (2025), a cooling network can be realized, connecting the heat island and cold island with a basis on circuit theory to organize cooling corridors and reduce SUHI intensity, towards climate resilient urban planning and organization.

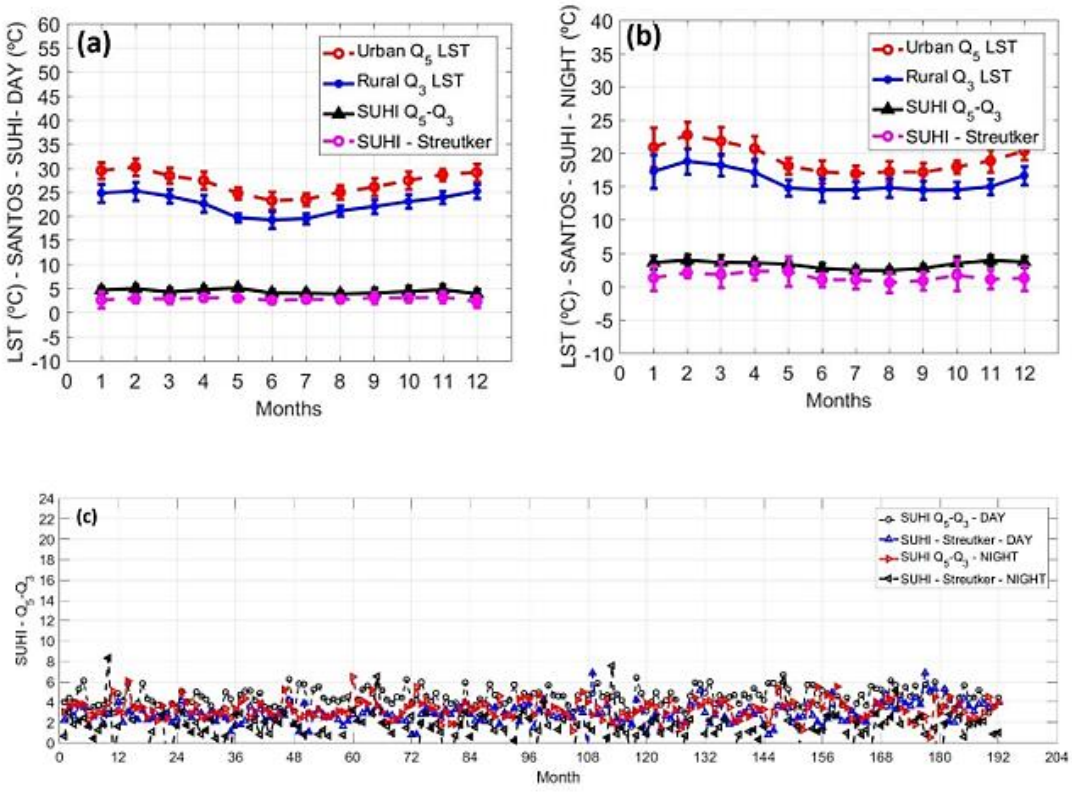

Fig. 4: (a) Time evolution from 2001-2020, monthly mean diurnal LST (°**C**) with standard deviation for diurnal period of urban LST (Q_5) rural LST (Q_3), SUHI intensity (°**C**) for CS, (b) night period. (c) Monthly evolution of SUHI by Streutker method and quantiles.

4. CONCLUSIONS

With the help of the data obtained from the MODIS sensor, the main objective was to estimate the SUHI during the period (2001-2020) at a resolution (0.05^0) for the CS, with the Streutker and quantile method, divided into 2 cases: urban and rural area separated with the help of the Land Cover Type MODIS product. According to the analysis and evidence presented in this paper, it was concluded:

The methods used for SUHI estimation in the diurnal period present little correlation between them, these have better fit during the nocturnal period. This could be explained by the existence of more than one center of maximum surface temperature during the day.

For the CS, during the diurnal periods, the SUHI intensity in May and August represent the maximum and minimum increase that could be reached within the urban area compared to rural areas. The nocturnal period presented maximum values in February and minimum values in August using the quantile method. In general, it was possible to show the formation of the heat island in the CS, with estimated increases greater than 5°C during the day and close to 4°C during the night. It is also recommended that future research use the MODIS sensor at higher spatial resolution and investigate urban planning strategies to mitigate the effects of heat islands.

5. PATENTS

Acknowledgments: The surface temperature data sets were obtained from NASA from their website at: http://modis.gsfc.nasa.gov/

Conflicts of Interest: The authors declare no conflicts of interest.

REFERENCES

[1]. Anees, S.A. *et al.* (2025) 'Spatiotemporal analysis of surface Urban Heat Island intensity and the role of vegetation in six major Pakistani cities', *Ecological Informatics*, 85, p. 102986. Available at: https://doi.org/10.1016/J.ECOINF.2024.102986.

[2]. Arnfield, A.J. (2003) 'Two decades of urban climate research: A review of turbulence, exchanges of energy and water, and the urban heat island', *International Journal of Climatology*, 23(1). Available at: https://doi.org/10.1002/joc.859.

[3]. Chen, H. *et al.* (2022) 'Influence of land cover change on spatio-temporal distribution of urban heat island —a case in Wuhan main urban area', *Sustainable Cities and Society*, 79, p. 103715. Available at: https://doi.org/10.1016/J.SCS.2022.103715.

[4]. Dai, Z., Guldmann, J.M. and Hu, Y. (2019) 'Thermal impacts of greenery, water, and impervious structures in Beijing's Olympic area: A spatial regression approach', *Ecological Indicators*, 97, pp. 77–88. Available at: https://doi.org/10.1016/J.ECOLIND.2018.09.041.

[5]. Dousset, B. and Gourmelon, F. (2003) 'Satellite multi-sensor data analysis of urban surface temperatures and landcover', in *ISPRS Journal of Photogrammetry and Remote Sensing*. Available at: https://doi.org/10.1016/S0924-2716(03)00016-9.

[6]. Du, Y. *et al.* (2025) 'Spatiotemporal Footprints of Surface Urban Heat Islands in the Urban Agglomeration of Yangtze River Delta During 2000–2022', *Remote Sensing 2025, Vol. 17, Page 892*, 17(5), p. 892. Available at: https://doi.org/10.3390/RS17050892.

[7]. Esposito, A. *et al.* (2024) 'Urban Morphology and Surface Urban Heat Island Relationship During Heat Waves: A Study of Milan and Lecce (Italy)', *Remote Sensing 2024, Vol. 16, Page 4496*, 16(23), p. 4496. Available at: https://doi.org/10.3390/RS16234496.

[8]. Feizizadeh, B. and Blaschke, T. (2013) 'Examining Urban heat Island relations to land use and air pollution: Multiple endmember spectral mixture analysis for thermal remote sensing', *IEEE Journal of Selected Topics in Applied Earth Observations and Remote Sensing*, 6(3), pp. 1749–1756. Available at: https://doi.org/10.1109/JSTARS.2013.2263425.

[9]. Flores R., J.L., Pereira Filho, A.J. and Karam, H.A. (2016) 'Estimation of long term low resolution surface urban heat island intensities for tropical cities using MODIS remote sensing data', *Urban Climate* [Preprint]. Available at: https://doi.org/10.1016/j.uclim.2016.04.002.

[10]. Fung, K.Y. *et al.* (2021) 'Comparing the Influence of Global Warming and Urban Anthropogenic Heat on Extreme Precipitation in Urbanized Pearl River Delta Area Based on Dynamical Downscaling', *Journal of Geophysical Research: Atmospheres*, 126(21), p. e2021JD035047. Available at: https://doi.org/10.1029/2021JD035047.

[11]. García, D.H. (2022) 'Analysis of Urban Heat Island and Heat Waves Using Sentinel-3 Images: a Study of Andalusian Cities in Spain', *Earth Systems and Environment*, 6(1), pp. 199–219. Available at: https://doi.org/10.1007/S41748-021-00268-9/METRICS.

[12]. Hardin, A.W. *et al.* (2018) 'Urban heat island intensity and spatial variability by synoptic weather type in the northeast U.S.', *Urban Climate*, 24, pp. 747–762. Available at: https://doi.org/10.1016/J.UCLIM.2017.09.001.

[13]. Holst, C.C., Tam, C.Y. and Chan, J.C.L. (2016) 'Sensitivity of urban rainfall to anthropogenic heat flux: A numerical experiment', *Geophysical Research Letters*, 43(5), pp. 2240–2248. Available at: https://doi.org/10.1002/2015GL067628.

[14]. Hu, C. *et al.* (2021) 'Urbanization Impacts on Pearl River Delta Extreme Rainfall Sensitivity to Land Cover Change Versus Anthropogenic Heat', *Earth and Space Science*, 8(3), p. e2020EA001536. Available at: https://doi.org/10.1029/2020EA001536.

[15]. Hurduc, A., Ermida, S.L. and DaCamara, C.C. (2024) 'On the Suitability of Different Satellite Land Surface Temperature Products to Study Surface Urban Heat Islands', *Remote Sensing*, 16(20), p. 3765. Available at: https://doi.org/10.3390/RS16203765/S1.

[16]. Iungman, T. *et al.* (2024) 'The impact of urban configuration types on urban heat islands, air pollution, CO2 emissions, and mortality in Europe: a data science approach', *The Lancet Planetary Health*, 8(7), pp. e489–e505. Available at: https://doi.org/10.1016/S2542-5196(24)00120-7.

[17]. Jacobs, C. *et al.* (2020) 'Are urban water bodies really cooling?', *Urban Climate*, 32, p. 100607. Available at: https://doi.org/10.1016/J.UCLIM.2020.100607.

[18]. Kazemi, A. *et al.* (2025) 'Temporal-spatial Distribution of Surface Urban Heat Island and Urban Pollution Island in an Industrial City: Seasonal Analysis', *IEEE Journal of Selected Topics in Applied Earth Observations and Remote Sensing* [Preprint]. Available at: https://doi.org/10.1109/JSTARS.2025.3541406.

[19]. Kim, Y.H. and Baik, J.J. (2005) 'Spatial and temporal structure of the urban heat island in Seoul', *Journal of Applied Meteorology*, 44(5). Available at: https://doi.org/10.1175/JAM2226.1.

[20]. Kolokotroni, M. *et al.* (2012) 'London's urban heat island: Impact on current and future energy consumption in office buildings', *Energy and Buildings*, 47. Available at: https://doi.org/10.1016/j.enbuild.2011.12.019.

[21]. Kuang, W.H. *et al.* (2017) 'An EcoCity model for regulating urban land cover structure and thermal environment: Taking Beijing as an example', *Science China Earth Sciences*, 60(6), pp. 1098–1109. Available at: https://doi.org/10.1007/S11430-016-9032-9/METRICS.

[22]. Luo, J., Zhu, L. and Fu, H. (2025) 'A new framework for mitigating urban heat island effect from the perspective of network', *Ecological Indicators*, 170, p. 113059. Available at: https://doi.org/10.1016/J.ECOLIND.2024.113059.

[23]. Ma, Z. *et al.* (2024) 'Evaluating Urban Heat Island Effects in the Southwestern Plateau of China: A Comparative Analysis of Nine Estimation Methods', *Land 2025, Vol. 14, Page 37*, 14(1), p. 37. Available at: https://doi.org/10.3390/LAND14010037.

[24]. Nandi, D. *et al.* (2024) 'Assessing urban heat island impact and identifying vulnerability zones through Geospatial and Geo-statistical techniques', *International Journal of Conservation Science*, 15(3), pp. 1577–1592. Available at: https://doi.org/10.36868/IJCS.2024.03.26.

[25]. Novio, R. *et al.* (2024) 'Study of Temporal Dynamics of Urban Heat Island Surface in Padang West Sumatra, Indonesia', *Nature Environment and Pollution Technology*, 23(2), pp. 1195–1200. Available at: https://doi.org/10.46488/NEPT.2024.v23i02.055.

[26]. Oke, T.R. (1982) 'The energetic basis of the urban heat island', *Quarterly Journal of the Royal Meteorological Society* [Preprint]. Available at: https://doi.org/10.1002/qj.49710845502.

[27]. Oke, T.R. (1987) *Boundary layer climates, Second edition, Inc.*

[28]. Oke, T.R. (1988) 'The urban energy balance', *Progress in Physical Geography*, 12(4), pp. 471–508. Available at: https://doi.org/10.1177/030913338801200401/ASSET/030913338801200401.FP.PNG_V03.

[29]. Ouyang, Z. *et al.* (2022) 'Albedo changes caused by future urbanization contribute to global warming', *Nature Communications 2022 13:1*, 13(1), pp. 1–9. Available at: https://doi.org/10.1038/s41467-022-31558-z.

[30]. Peng, J. *et al.* (2024) 'Diversified evolutionary patterns of surface urban heat island in new expansion areas of 31 Chinese cities', *npj Urban Sustainability 2024 4:1*, 4(1), pp. 1–11. Available at: https://doi.org/10.1038/s42949-024-00152-1.

[31]. Roth, M. (2007) 'Review of urban climate research in (sub)tropical regions', in *International Journal of Climatology*. Available at: https://doi.org/10.1002/joc.1591.

[32]. Schneider, A. *et al.* (2003) 'Mapping Urban Areas by Fusing Multiple Sources of Coarse Resolution Remotely Sensed Data', *Photogrammetric Engineering and Remote Sensing*. Available at: https://doi.org/10.14358/PERS.69.12.1377.

[33]. Shahmohamadi, P. *et al.* (2011) 'The Impact of Anthropogenic Heat on Formation of Urban Heat Island and Energy Consumption Balance', *Urban Studies Research*, 2011(1), p. 497524. Available at: https://doi.org/10.1155/2011/497524.

[34]. Shapiro, A.D. and Liu, W. (2023) 'Evaluating Land Surface Temperature Trends and Explanatory Variables in the Miami Metropolitan Area from 2002–2021', *Geomatics*, 4(1), pp. 1–16. Available at: https://doi.org/10.3390/GEOMATICS4010001/S1.

[35]. Soltani, A. and Sharifi, E. (2017) 'Daily variation of urban heat island effect and its correlations to urban greenery: A case study of Adelaide', *Frontiers of Architectural Research*, 6(4), pp. 529–538. Available at: https://doi.org/10.1016/J.FOAR.2017.08.001.

[36]. Streutker, D.R. (2003) 'Satellite-measured growth of the urban heat island of Houston, Texas', *Remote Sensing of Environment*, 85(3). Available at: https://doi.org/10.1016/S0034-4257(03)00007-5.

[37]. Suazo, J.M.A. *et al.* (2019) 'Estimation of superficial urban heat island in the metropolitan area of Iquitos[Estimación de Isla de Calor Urbana Superficial en el Area Metropolitana de Iquitos/Peru]', *Anuario do Instituto de Geociencias*, 42(1), pp. 135–145. Available at: https://doi.org/10.11137/2019_1_135_145.

[38]. Suazo, J.M.A., Rojas, J.L.F. and Karam, H.A. (2020) 'Isla de Calor Urbana Superficial para Tres Megaciudades en África', *Anuário do Instituto de Geociências - UFRJ* [Preprint]. Available at: https://doi.org/10.11137/2020_2_64_75.

[39]. Suthar, G. *et al.* (2023) 'Spatiotemporal variation of air pollutants and their relationship with land surface temperature in Bengaluru, India', *Remote Sensing Applications: Society and Environment*, 32, p. 101011. Available at: https://doi.org/10.1016/J.RSASE.2023.101011.

[40]. Voogt, J.A. and Oke, T.R. (2003) 'Thermal remote sensing of urban climates', *Remote Sensing of Environment* [Preprint]. Available at: https://doi.org/10.1016/S0034-4257(03)00079-8.

[41]. Wang, Z. *et al.* (2021) 'The projected effects of urbanization and climate change on summer thermal environment in Guangdong-Hong Kong-Macao Greater Bay Area of China', *Urban Climate*, 37, p. 100866. Available at: https://doi.org/10.1016/J.UCLIM.2021.100866.

[42]. Wan, Z. (1999) *MODIS land-surface temperature algorithm theoretical basis document (LST ATBD). Institute for Computational Earth System Science, Santa Barbara., Institute for Computational Earth System Science University ofCalifornia*.

[43]. Wan, Z. and Li, Z.L. (1997) 'A physics-based algorithm for retrieving land-surface emissivity and temperature from eos/modis data', *IEEE Transactions on Geoscience and Remote Sensing*, 35(4). Available at: https://doi.org/10.1109/36.602541.

[44]. Wu, X., Zhang, L. and Zang, S. (2019) 'Examining seasonal effect of urban heat island in a coastal city', *PLOS ONE*, 14(6), p. e0217850. Available at: https://doi.org/10.1371/JOURNAL.PONE.0217850.

[45]. Yao, R. *et al.* (2018) 'The influence of different data and method on estimating the surface urban heat island intensity', *Ecological Indicators*, 89, pp. 45–55. Available at: https://doi.org/10.1016/J.ECOLIND.2018.01.044.

[46]. You, M. *et al.* (2021) 'Quantitative Analysis of a Spatial Distribution and Driving Factors of the Urban Heat Island Effect: A Case Study of Fuzhou Central Area, China', *International Journal of Environmental Research and Public Health 2021, Vol. 18, Page 13088*, 18(24), p. 13088. Available at: https://doi.org/10.3390/IJERPH182413088.

[47]. Zargari, M. *et al.* (2024) 'Climatic comparison of surface urban heat island using satellite remote sensing in Tehran and suburbs', *Scientific Reports 2024 14:1*, 14(1), pp. 1–23. Available at: https://doi.org/10.1038/s41598-023-50757-2.